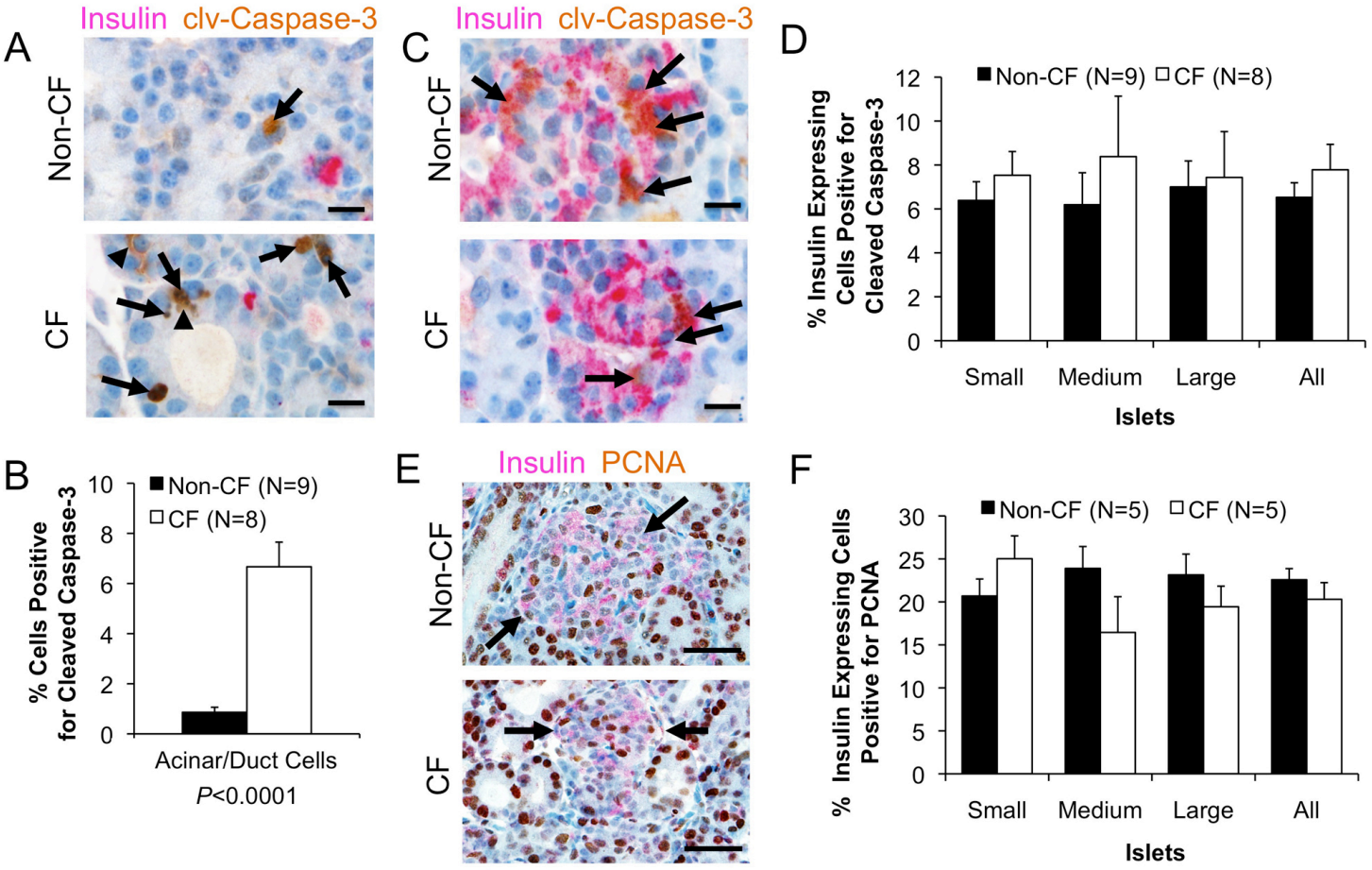

Supplemental Figure S1. Apoptosis and proliferation in newborn CF and non-CF ferret pancreata. (A) Representative images of cleaved caspase-3 (clv-Caspase-3) immunostaining (brown) in acinar/duct regions of non-CF and CF newborn pancreata. Sections were dual stained for insulin (pink). Staining is present within apoptotic bodies (arrows) and cytoplasm (arrowhead) of acinar/duct cells (Bar=20μm). (B) Cleaved caspase-3 scoring in acinar/duct cells. (C) Representative images of cleaved caspase-3 (brown) and insulin (pink) dual stained sections in regions containing islets (arrows indicate cells positive for both cleaved caspase-3 and insulin) (Bar=20μm). (D) Cleaved caspase-3 scoring in various islet sizes (small, medium, large) and all islets. (E) Representative images of PCNA (brown nuclei) and insulin (pink) dual stained sections (arrows define the islet boundaries) (Bar=50μm). (F) PCNA scoring in various islet sizes (small, medium, large) and all islets. Graphs represent the mean +/- SEM, with N number of independent animals evaluated. *P* value in panel B was determined using the nonparametric two-tailed Mann-Whitney test. There were no significant differences between genotypes for comparisons between various sized islets panels D and F using Kruskal-Wallis non-parametric one-way ANOVA with a Dunn's post-test. All islet sizes grouped together were analyzed by the nonparametric two-tailed Mann-Whitney test and were also not significantly different between genotypes (Panel D P=0.3258; Panel D P=0.2998).

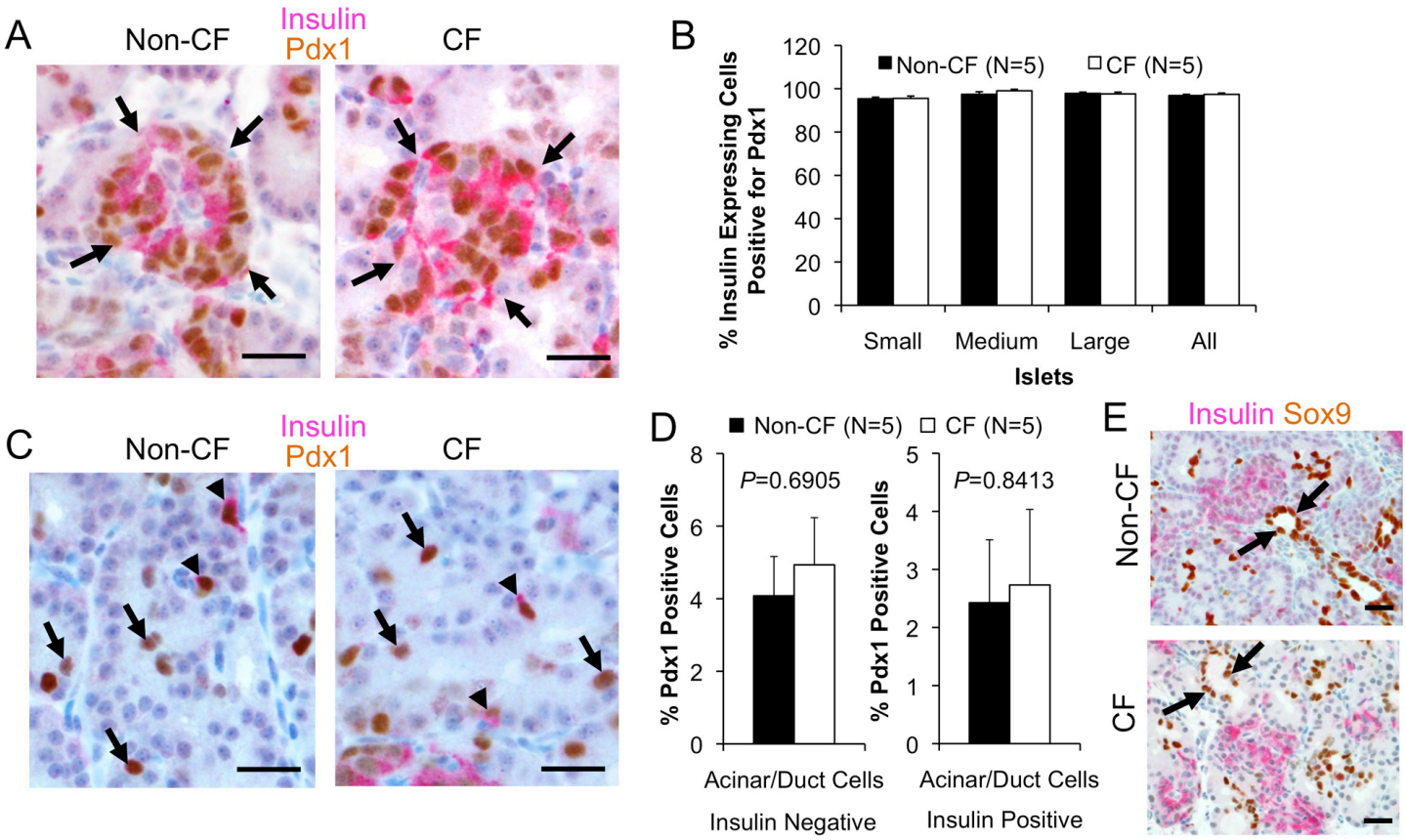

Supplemental Figure S2. Pdx1 and SOX9 expression in newborn CF and non-CF ferret pancreata. (A) Representative images of Pdx1 (brown nuclei) and insulin (pink cytoplasm) dual staining in islets (islet boundary is marked by arrows) of non-CF and CF newborn pancreata (Bar=25μm) (B) Quantification of Pdx1 expression in insulin positive cells of various islet sizes (small, medium and large) and all islets. (C) Representative images of Pdx1 and insulin dual staining demonstrating Pdx1 immunoreactivity in insulin negative (arrows) and insulin positive (arrowheads) acinar/duct cells (Bar=25μm). (D) Quantification of % $Pdx1^{+}$/$insulin^{-}$ and $Pdx1^{+}$/$insulin^{+}$ cells in acinar/duct regions as the fraction of total nuclei. (E) Representative images of SOX9 (brown nuclei) and insulin (pink cytoplasm) dual stained non-CF and CF newborn pancreata. Arrows mark the boundary of ducts. Graphs represent the mean +/-SEM, with N number of independent animals evaluated. There were no significant differences between genotypes for comparisons between various sized islets panel B using Kruskal-Wallis non-parametric one-way ANOVA with a Dunn's post-test. All islet sizes grouped together were analyzed by the nonparametric two-tailed Mann-Whitney test and were also not significantly different between genotypes (Panel B *P*=0.4538). *P* values shown in panel D were determined using the nonparametric two-tailed Mann-Whitney test.

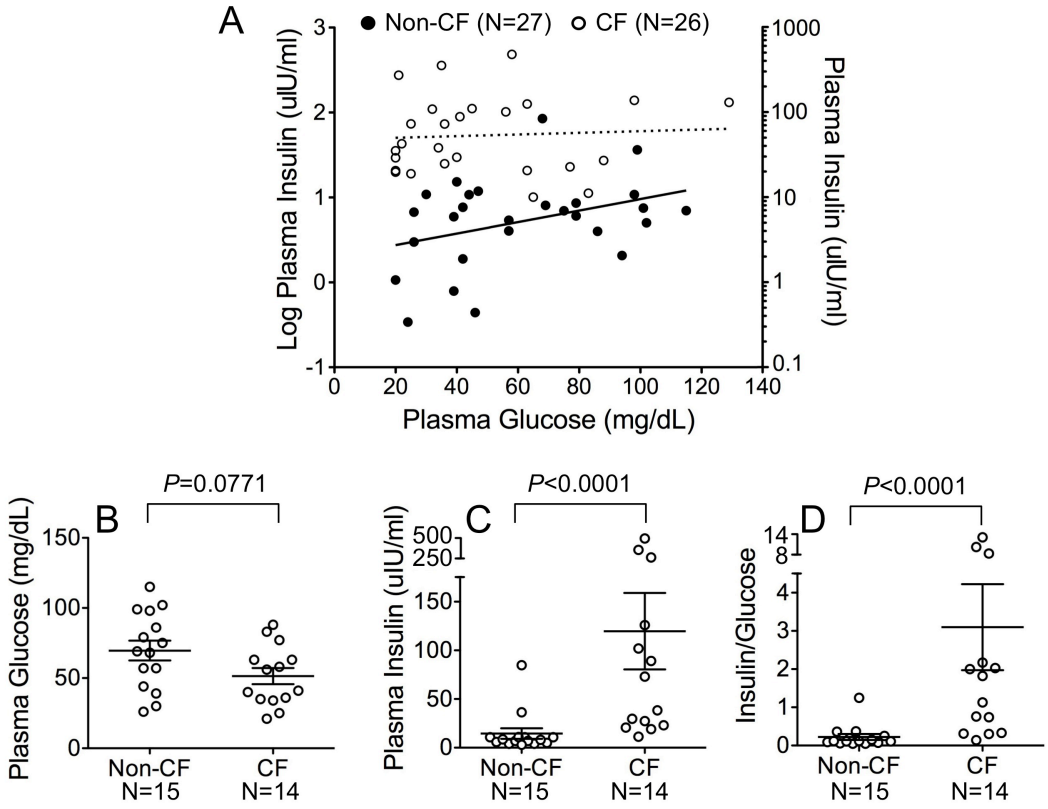

Supplemental Figure S3. Abnormalities in insulin secretion occur in newborn nursing CF ferrets. This supplement is an extension of Figure 9. (A) Blood glucose versus log[insulin] is shown by genotype, with the best fit linear regressions. The data points are from animals shown in Figure 9A and B. For the non-CF data, the slope (0.00677 log[μU insulin/ml]/[mg/dL glucose]) of the line was non-zero (P<0.0468, N=27 animals), whereas for the CF group the slope (0.00097 log[μU insulin/ml]/[mg/dL glucose]) was not significantly different than zero (P=0.7743, N=26 animals). For the non-CF data, y-intercept (0.304 log[μU insulin/ml]) was not significantly greater than zero (P=0.1774), whereas for the CF group the y-intercept (1.68 log[μU insulin/ml]) was significantly greater than zero (P<7.04 x 10^{-12}). Statistical analysis of regression slopes and intercepts used the linear model function in R (http://www.R-project.org). The right y-axis is for easy-to-read reference only, all statistical analyses were performed in insulin log space. (B-D) This supplement depicts the plasma glucose, insulin, and insulin/glucose data from the cohort of animals evaluated in Figure 9G-I for C-peptide. Values for all graphs show the mean +/-SEM for N independent animals. Significant differences in all panels were assessed using a nonparametric two-tailed Mann-Whitney test (P values are shown on each graph). Significantly higher variances in CF, as compared to non-CF, values of panels B and C were observed by F-test (P<0.0001). Variances were not significantly different between genotypes for panels A.

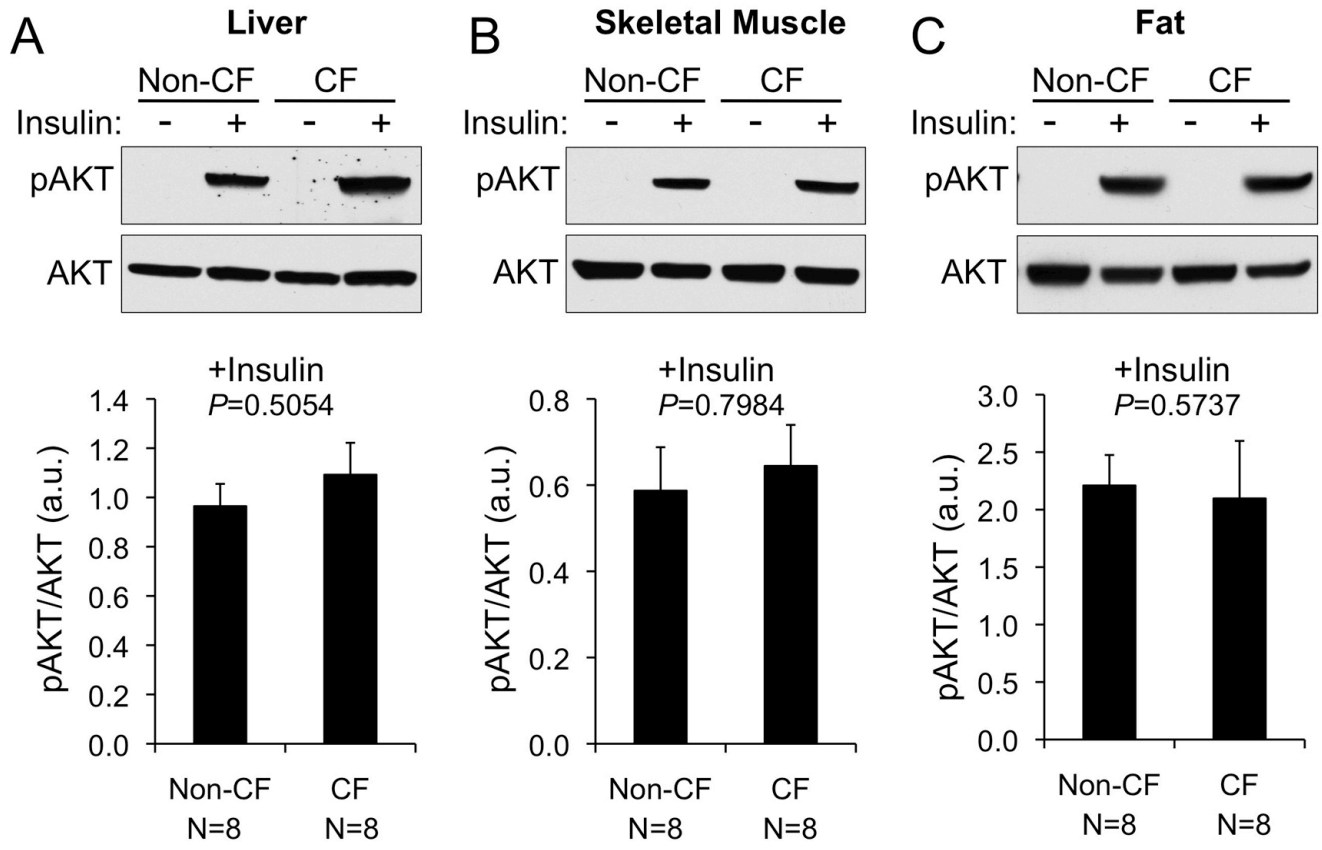

Supplemental Figure S4. Insulin sensitivity in newborn ferrets. (A-B) Relative insulin-stimulated AKT phosphorylation (serine 473) in newborn CF and non-CF ferrets was evaluated in (A) liver, (B) skeletal muscle, and (C) perirenal fat following administration of intravenous insulin. Top panels are representative immunoblots of phosphorylated and total AKT from tissues of newborn ferrets with and without insulin injection. Graphs in the bottom panels represent the mean +/-SEM ratio of pAKT/AKT intensities of immunoreactivity as assessed using NIH Image J for N independent animals. *P* values in the lower panels were determined using the nonparametric two-tailed Mann-Whitney test.

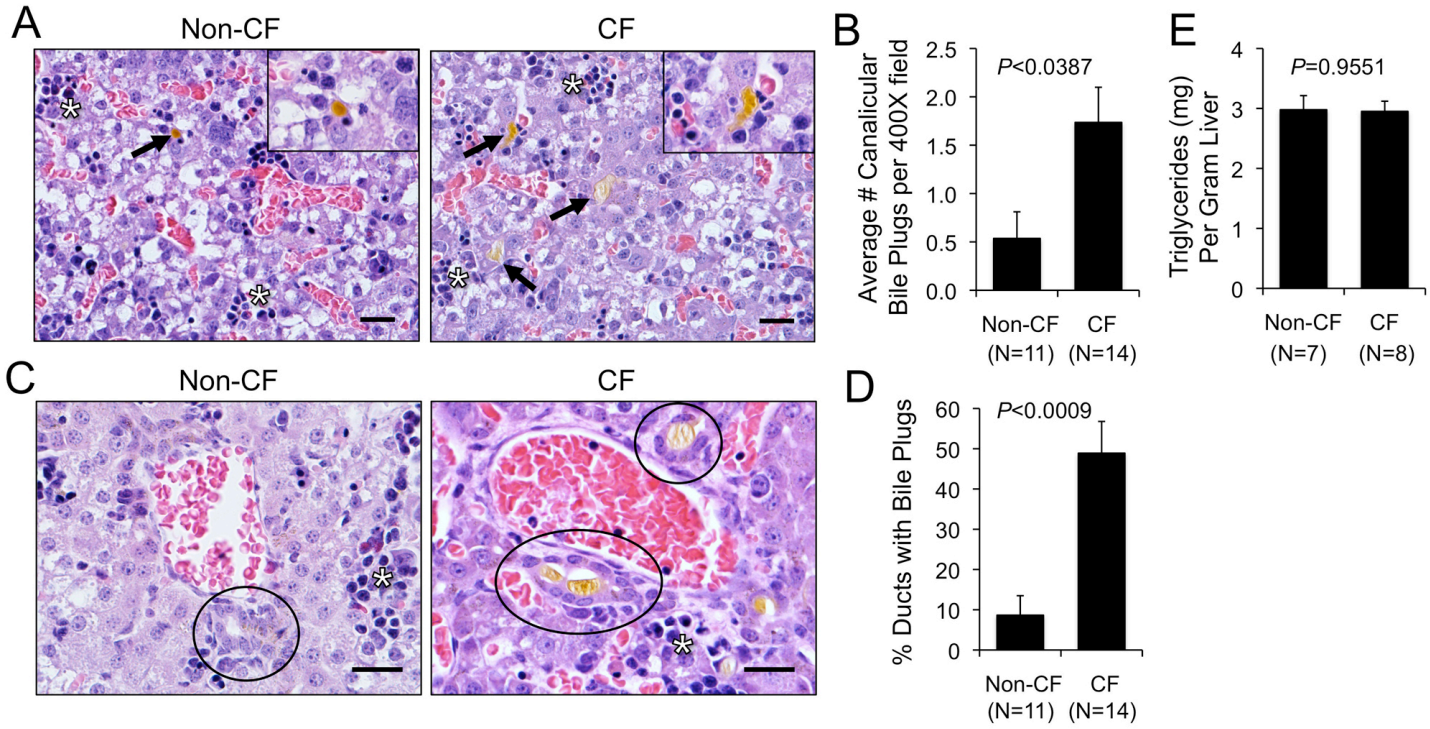

Supplemental Figure S5. Analysis of hepatic bile plugging and total triglycerides in newborn CF and non-CF ferrets. (A) Representative images of bile canalicular plugs (arrows) in non-CF and CF liver. The inset is a higher magnification of one of the arrows to illustrate the brown granular bile plug (Bar=25 μm). (B) Average number of canalicular bile plugs per 400X field in non-CF and CF livers. (C) Representative images of bile ducts (circled) without a bile plug (non-CF) and with a bile plug (CF) (Bar=25 μm). (D) The % of bile ducts with bile plugs in non-CF and CF livers. (E) Total triglycerides in newborn non-CF and CF livers. Values for all graphs show the mean +/-SEM for N independent animals. *P* values in panels B, D, and E were determined using the nonparametric two-tailed Mann-Whitney test (*P* values are shown on each graph). Asterisks in panels A and C mark areas of extramedullary hematopoiesis commonly observe in both genotypes.

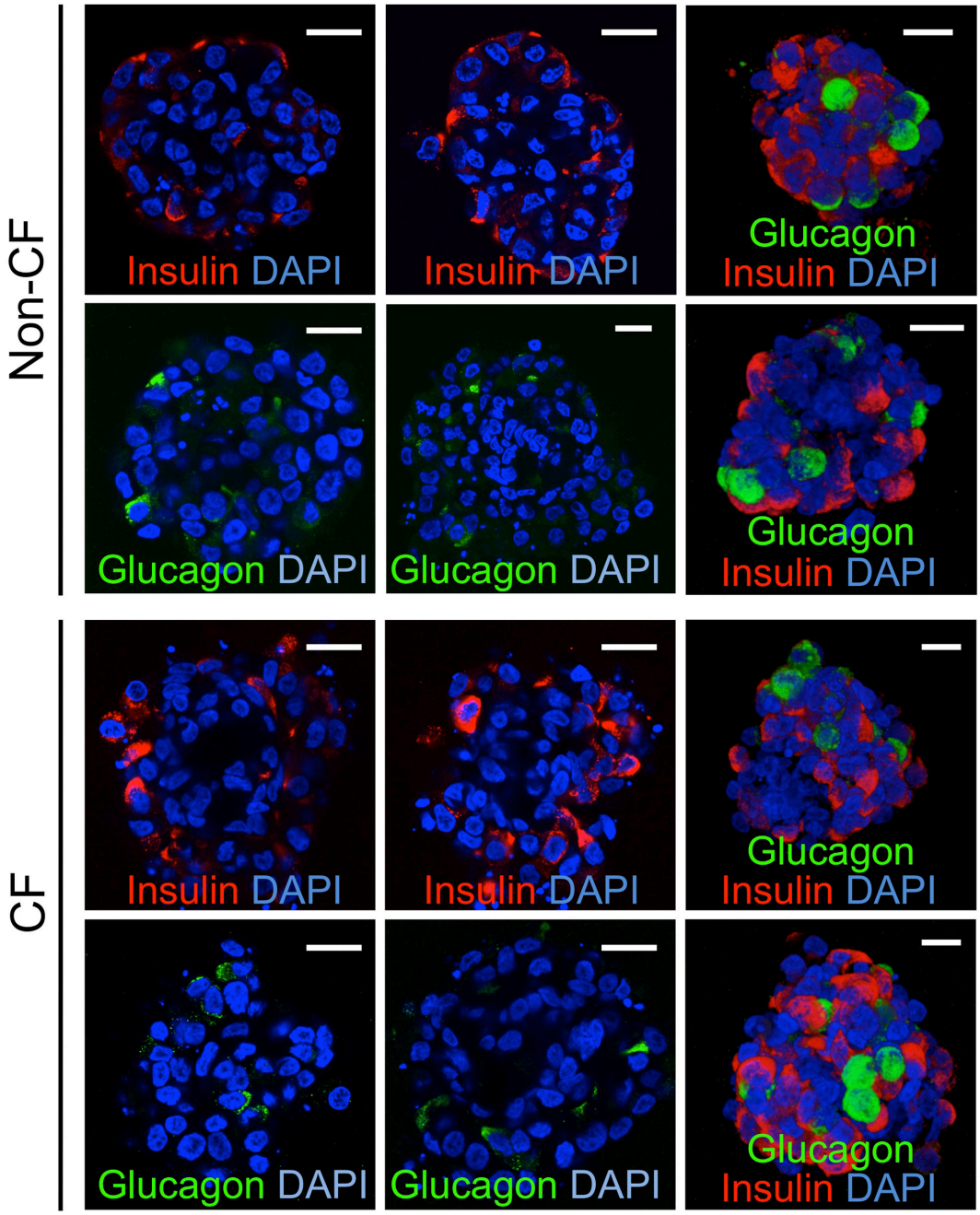

Supplemental Figure S6. Newborn 9 day cultures of CF and non-CF ferret islets were fixed in 4% paraformaldehyde for 4 hours at 4°C, followed by rinsing in PBS. Immunofluorescent staining for insulin and/or glucagon were performed on whole-mount samples following blocking in 10% donkey serum/PBS containing 0.5% Triton-X-100. Single antigen localization was performed on islet suspensions, while islets used for 3D rendering and co-localization were followng embedding in Matrigel (BD Biosciences) to enhance retention of 3D structure. Primary antibodies used for immunostaining include guinea pig anti-insulin at a 1:500 dilution (MP Biomedicals) and rabbit anti-glucagon at a 1:500 dilution (MP Biomedicals). The secondary antibodies included rhodamine red-conjugated donkey anti-guinea pig at a 1:250 dilution (Jackson ImmunoResearch) and FITC-conjugated donkey anti-rabbit at a 1:250 dilution (Jackson ImmunoResearch). Following staining, samples were rinsed in PBS and then placed in Vectashield Mounting Medium (Vector Labs) containing DAPI to mark nuclei prior to laser scanning confocal microscopy (Zeiss 700). The left and middle columns of photomicrographs representative confocal slices through the center of independent islets from each genotype singly stained for insulin or glucagon. The right column of photomicrographs representative confocal 3D renderings of independent islets from each genotype co-stained for insulin or glucagon. Scale bar = 25μm.